Electrochemical deposition of platinum within nanopores on silicon: Drastic acceleration originating from surface-induced phase transition

Kazuhiro Fukami, Ryo Koda, Tetsuo Sakka, Yukio Ogata, and Masahiro Kinoshita

Citation: The Journal of Chemical Physics **138**, 094702 (2013); doi: 10.1063/1.4793526
View online: http://dx.doi.org/10.1063/1.4793526
View Table of Contents: http://scitation.aip.org/content/aip/journal/jcp/138/9?ver=pdfcov
Published by the AIP Publishing

Electrochemical deposition of platinum within nanopores on silicon: Drastic acceleration originating from surface-induced phase transition

Kazuhiro Fukami,[a] Ryo Koda, Tetsuo Sakka,[b] Yukio Ogata, and Masahiro Kinoshita[c]
Institute of Advanced Energy, Kyoto University, Uji, Kyoto 611-0011, Japan

(Received 19 November 2012; accepted 12 February 2013; published online 6 March 2013)

An electrochemical reaction within nanopores is remarkably decelerated once a diffusion-limited condition is reached due to the difficulty in supply of reactants from the bulk. Here, we report a powerful method of overcoming this problem for electrochemical deposition of platinum within nanopores formed on silicon. We made the pore wall surface of the silicon electrode hydrophobic by covering it with organic molecules and adopted platinum complex ions with sufficiently large sizes. Such ions, which are only weakly hydrated, are excluded from the bulk aqueous electrolyte solution to the surface and rather hydrophobic in this sense. When the ion concentration in the bulk was gradually increased, at a threshold the deposition behavior exhibited a sudden change, leading to drastic acceleration of the electrochemical deposition. Using our statistical-mechanical theory for confined molecular liquids, we show that this change originates from a surface-induced phase transition: The space within nanopores is abruptly filled with the second phase within which the ion concentration is orders of magnitude higher. When the affinity of the surface with water was gradually reduced with fixing the ion concentration, qualitatively the same transition phenomenon was observed, which can also be elucidated by our theory. The utilization of the surface-induced phase transition sheds new light on the design and control of a chemical reaction in nanospace. © *2013 American Institute of Physics*. [http://dx.doi.org/10.1063/1.4793526]

I. INTRODUCTION

Porous electrodes have become important materials in science and technology. They are utilized as sensing devices, host matrices for catalysts, and electrodes for batteries.[1–6] Although the specific surface area becomes larger with an increase in the porosity, it is difficult in chemical or electrochemical reactions to elicit suitably high performance originating from the large specific surface area. This is because the reaction efficiency within nanoporous media is lowered by the difficulty in supply of reactants from the bulk and in ejection of products to the bulk. By applying the diffusion equation to the description of supply and ejection, we know that they are strongly disturbed by the porous structure and this disturbance is more serious whose pores are deeper and smaller in diameter.[7] As a consequence, chemical or electrochemical reactions occur primarily on the top surface of porous structure which is advantageous in terms of supply of reactants from the bulk. Thus, the control of such reactions within nanoporous media is much more difficult than one simply imagines.

It was reported that the local structure of ionic liquid or organic solvent in a confined nanospace is substantially different from that in the bulk.[8–10] Recently, we have revealed experimentally and theoretically that the surface-induced hydration structure of platinum complex ions has large effects on the enhancement of platinum deposition within nanoporous silicon electrodes.[11] The surface-induced hydration structure plays crucially important roles in the design and control of chemical reactions in nanoporous electrodes. When the pore wall surface was made hydrophobic and platinum complex ions with sufficiently large sizes were adopted, the ion concentration was greatly enriched at the surface due to rather hydrophobic properties of the ions. Since such large ions are only weakly hydrated, they are excluded from the bulk to the surface and rather hydrophobic in this sense. (As the anion size becomes larger with its charge kept constant, hydrogen atoms in a water molecule with positive partial charges cannot come closer to it, leading to weaker stabilization by the electrostatic attractive interaction. That is, a larger anion exhibits weaker affinity with water and becomes less hydrophilic.) However, it was reported that the structure had only monolayer thickness of the ions. In such a case, it was not clear how the diffusion limitation of reactants was overcome in the confined nanospace (i.e., nano-sized pores).

In the present study, we carry out a detailed investigation on the effects due to the concentration of platinum complex ions in the bulk aqueous electrolyte solution and the affinity of the pore wall surface with water. A surprising finding is as follows. When the ion concentration in the bulk was gradually increased, at a threshold concentration the deposition behavior exhibited a sudden change, leading to drastic acceleration of the electrochemical deposition. This result is strongly suggestive of the occurrence of a transition phenomenon. When the affinity of the surface with water was gradually reduced (i.e., the hydrophobicity of the surface was gradually strengthened) with fixing the ion concentration, qualitatively the same phenomenon was observed. With the aid of our

[a]Electronic mail: fukami.kazuhiro.2u@kyoto-u.ac.jp.
[b]Present address: Department of Energy and Hydrocarbon Chemistry, Graduate School of Engineering, Kyoto University, Nishikyo-ku, Kyoto 615-8510, Japan.
[c]Electronic mail: kinoshit@iae.kyoto-u.ac.jp.

statistical-mechanical theory for confined molecular liquids, we attribute the finding to a surface-induced phase transition upon which the confined nanospace is filled with the second phase: The ion concentration is orders of magnitude higher in the second phase. We emphasize that the bulk aqueous electrolyte solution is thermodynamically stable as a single phase and subject to no phase transition. The transition in the present case is induced by the surface. A liquid mixture confined in nanospace behaves quite differently from the bulk. Thus, we have newly found that the elimination of the diffusion-limited condition, under which supply of reactants (i.e., platinum complex ions) from the bulk to nanospace is remarkably decelerated, originates not from the simple enrichment of the reactants at the surface but from the surface-induced phase transition. The theoretical analysis in our earlier work[11] was made only for a very low ion concentration which was far from the threshold for the phase transition.

In the present paper, we first present the striking experimental results of the electrochemical deposition behavior within porous silicon electrodes whose pore diameter is ~3 nm on an average, showing the existence of thresholds for the concentration of platinum complex ions in the bulk and the affinity of pore wall surface with water. Beyond the threshold, the drastic acceleration of platinum deposition within the porous layer is clearly observed from the density distribution of the platinum deposit. We then perform theoretical analyses based on statistical mechanics for confined molecular liquids to elucidate the experimental results. It is shown that the transition behavior with thresholds is semi-quantitatively reproduced in the analyses, suggesting that the surface-induced phase transition is responsible for the drastic acceleration of platinum deposition. To the best of our knowledge, a surface-induced phase transition has never been reported for an aqueous electrolyte solution near a hydrophobic surface, which contains only weakly hydrated ions. Moreover, it is the first time that a surface-induced phase transition is clearly visualized in electrodeposition within porous silicon and studied by a combination of experimental and theoretical approaches. The present work is expected to stimulate the progress of an interesting new field, i.e., chemical physics of a liquid or liquid mixture confined in nanospace. It will also have a strong impact not only on the fundamental understanding of such reactions within nanopores but also on the design and control of the reactions in nanoporous media. We believe that the surface-induced phase transition will play essential roles in the adjustment of the distribution of chemicals within nanopores, enabling precise control of materials, such as fast response time of sensors, high efficiency of catalytic reactions, and quick recharge of batteries.

II. MATERIALS AND METHODS

Porous silicon electrodes were prepared by anodization of p-type silicon (100) with a resistivity of 10–20 Ω cm. The diameters of the pores were less than 5 nm, and the average diameter was ~3 nm. The anodization was carried out in HF/ethanol solution under a constant current density of 2.0 mA cm^{-2}. The duration for the electrochemical dissolution of silicon was tuned so that two porous layers different in thickness could be obtained. A thicker layer possesses deeper pores, and we can explore the effect of pore depth. The porous silicon electrode was dipped into *n*-hexane containing methyl propiolate (hydrophobic) and/or propiolic acid (hydrophilic). To obtain a hydrophobic porous silicon electrode, *n*-hexane solution of 0.2 M methyl propiolate without propiolic acid was used, and for the hydrophilic nanoporous silicon the recipe was the other way around.[11] Mixture of methyl propiolate and propiolic acid prepared at different relative concentrations was used to adjust the affinity of the pore wall surface with water (i.e., to change the degree of hydrophilicity or hydrophobicity). Details are written in the caption of each figure.

Electrochemical deposition of platinum using the hydrophobic and hydrophilic porous silicon electrodes was performed at a constant current density of $-6.4\ \mu A\ cm^{-2}$ (the minus sign means the cathodic current density). Aqueous electrolyte solution of K_2PtCl_4 and 0.5 M NaCl was used as the deposition bath. In some cases, aqueous electrolyte solution of K_2PtBr_4 and 0.5 M KBr was used instead of the chloride bath. The platinum complex ions are $[PtCl_4]^{2-}$ and $[PtBr_4]^{2-}$. Concentrations of the platinum sources were tuned from 0.001 M to 0.1 M. The cross-sectional views of the nanoporous silicon were observed by a field-emission type scanning electron microscope (JEOL JSM-6500F).

III. EXPERIMENTAL RESULTS

A. Effect of concentration of platinum complex ions

Using the pore wall surface modified only with methyl propiolate to make it hydrophobic, we investigated the effect of the concentration of platinum complex ions on the deposition behavior. Electrochemical deposition of platinum was performed with gradually increasing the concentration of $[PtCl_4]^{2-}$ from 0.001 M (the increment was 0.001 M). A drastic change in the deposition behavior was observed at a threshold concentration: The behavior for 0.010 M becomes markedly different from that for 0.009 M. The drastic change can be appreciated from Figures 1(b) and 1(c). Platinum deposition is not observed at all within the porous layer when the ion concentration is 0.009 M or lower. In contrast, platinum is uniformly distributed in the nanoporous silicon electrode when the ion concentration is 0.010 M or higher. The microscopic structure of the platinum deposited is the same as that reported in our previous paper. Namely, platinum was deposited not as continuous platinum fibers but as isolated nanometer-sized particles. Thus, there exists a threshold (between 0.009 M and 0.010 M) in the concentration of $[PtCl_4]^{2-}$ for the deposition within the nanoporous layer. We note that the amount of platinum deposited is constant under the present experimental condition. Even if the electrochemical deposition within the porous layer is suppressed, the same amount of platinum is deposited mostly on the top surface of the porous layer.

Our earlier work showed that the electrochemical deposition of platinum in the porous silicon electrodes is remarkably enhanced when $[PtCl_4]^{2-}$ is replaced by $[PtBr_4]^{2-}$. This is because larger ions become more hydrophobic and tend to be

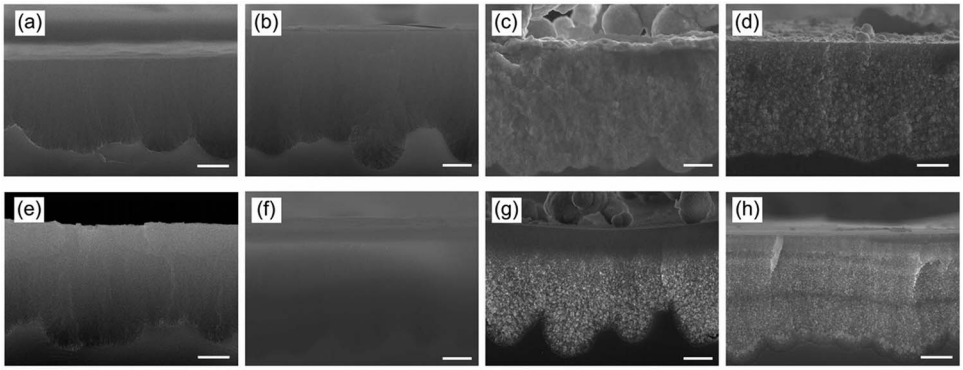

FIG. 1. Cross-sectional SEM images of the porous silicon electrodes after electrochemical deposition of platinum. The electrochemical deposition was carried out in the $[PtCl_4]^{2-}$ and $[PtBr_4]^{2-}$ baths for (a)–(d) and (e)–(h), respectively. Concentrations of platinum ions were (a) 0.001 M, (b) 0.009 M, (c) 0.010 M and (d) 0.100 M for $[PtCl_4]^{2-}$, and (e) 0.002 M, (f) 0.004 M, (g) 0.005 M and (h) 0.100 M for $[PtBr_4]^{2-}$. The drastic change in the electrodeposition within the porous layer can be appreciated from (b) and (c) for $[PtCl_4]^{2-}$ and from (f) and (g) for $[PtBr_4]^{2-}$. White bars in the figures indicate 0.5 μm.

excluded from the bulk to a hydrophobic surface to a stronger extent. The effect of ion size on the deposition behavior is revisited in the present study. Figures 1(e)–1(h) depict the deposition behavior observed after the electrochemical deposition using $[PtBr_4]^{2-}$. There also exists a threshold in the concentration of $[PtBr_4]^{2-}$ between 0.004 M and 0.005 M which is considerably lower than in the case of $[PtCl_4]^{2-}$ (Figs. 1(f) and 1(g)).

B. Effect of affinity of pore wall surface with water

The surface-induced structure of platinum complex ions is dependent upon the affinity of the pore wall surface with water. In this experiment, the concentration of $[PtCl_4]^{2-}$ was kept constant at 0.1 M, but the affinity was controlled by modifying the surface in mixture *n*-hexane solutions of methyl propiolate and propiolic acid with various molar ratios. The total concentration of methyl propiolate and propiolic acid was kept constant at 0.2 M. When the porous electrode modified with 0.13 M methyl propiolate and 0.07 M propiolic acid was used, no platinum deposited was observed in the porous layer as shown in Figure 2(a). Platinum can be observed on the top surface of the porous layer (or slightly inside the porous layer from the top). This electrode had the contact angle of 83° with ultra pure water before the electrochemical deposition (Figure 2(c)). Interestingly, the deposition behavior showed a drastic change when the electrode was modified with 0.14 M methyl propiolate and 0.06 M propiolic acid. Because the relative concentration of propiolic acid was slightly higher, the contact angle exhibited only a minor increase from 83° to 86° as shown in Figure 2(d). The deposition behavior for 86° becomes markedly different (i.e., an abrupt change is displayed) from that for 83°. The electrochemical deposition within the porous layer was promoted far more strongly when the porous electrode with the contact angle of 86° was used (Figure 2(b)). The very small increase in the contact angle or in the surface hydrophobicity is effective enough to induce such a drastic change in the deposition behavior. Again, there exists a threshold degree of the affinity of the pore wall surface with water.

C. Effect of depth of nanopores

We investigate the effect of pore depth on the electrochemical deposition behavior for the hydrophobic surface. If supply of the ions was made through mass transfer, the deposition behavior would be influenced by the pore depth. The pore depth (or equivalently, the thickness of the porous layer) can be tuned by changing the anodization time for preparing the porous silicon electrodes. Although the porous-layer thickness (i.e., the pore depth) of ~2 μm in the experiment described above could be sufficiently large, a silicon electrode with even much deeper pores (the thickness reaches ~5 μm) was also tested in the $[PtCl_4]^{2-}$ or $[PtBr_4]^{2-}$ bath. The concentration of the platinum complex ions was 0.1 M. As shown in Figure 3, for both of $[PtCl_4]^{2-}$ and $[PtBr_4]^{2-}$, platinum is uniformly deposited and distributed within the pores as in the case of shallow pores. Surprisingly, no voids are found in the deposit. The amount of platinum deposited on the top surface is smaller for $[PtBr_4]^{2-}$ than for $[PtCl_4]^{2-}$, which is

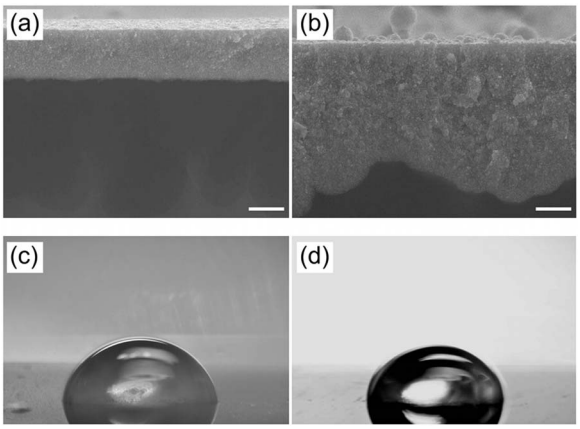

FIG. 2. Cross-sectional SEM images (a) and (b) of the porous silicon electrodes modified with both propiolic acid and methyl propiolate under different molar ratios. Images shown in (c) and (d) are snapshots of contact angle measurements. Concentrations of propiolic acid and methyl propiolate were 0.07 M and 0.13 M, respectively, for (a) and (c), while they were 0.06 M and 0.14 M, respectively, for (b) and (d). The electrodes shown in (a) and (c) were only slightly more hydrophilic than those shown in (b) and (d). The cross-sectional images were taken after electrochemical deposition of platinum. White bars in the figures (a) and (b) indicate 0.5 μm.

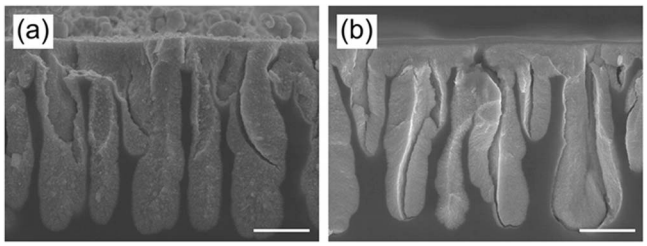

FIG. 3. Cross-sectional SEM images of thicker porous silicon electrodes after electrochemical deposition of platinum. The electrochemical deposition was carried out in the $[PtCl_4]^{2-}$ and $[PtBr_4]^{2-}$ baths for (a) and (b), respectively. The concentration of the platinum complex ions was 0.1 M. The thickness of the porous layer was ~5 μm. White bars in the figures indicate 2 μm.

independent of the pore depth. From these results, we can conclude that supply of the ions is made not through mass transfer but through another physical factor.

D. Summary of experimental results

We have found that there exists a threshold for the concentration of platinum complex ions. The behavior of platinum deposition within nanopores on silicon falls into one of two completely distinct categories in terms of whether the concentration is lower or higher than the threshold. This result is strongly suggestive of the occurrence of a transition phenomenon. A threshold degree of the affinity of the pore wall surface with water also exists. Once the ion concentration or the degree of surface hydrophobicity exceeds the threshold, drastic acceleration of the electrochemical deposition occurs within nanometer-sized pores irrespective of their depth. The existence of such thresholds cannot be explained by the simple consideration of the electrochemical reaction coupled with mass transfer. It should be noted that porous silicon with ~20 nm in diameter could be fabricated by electrochemical dissolution of highly doped silicon wafers. However, the pore size is considerably dependent on the doping level, and the electrodeposition behavior becomes different between ~2 nm-sized pores and ~20 nm-sized pores in terms of electrochemical properties. Hence, it is not straightforward to examine the pore-size effect from an experimental viewpoint.

In earlier work, we gave the following remarks: The surface-induced hydration structure of platinum ions is crucial for controlling the electrochemical deposition; the ion concentration is enriched within a thin layer (its thickness is almost equal to the ion size) at the surface; but the average ion concentration within the layer increases only in proportion to the bulk concentration. Hence, the existence of such thresholds cannot be explained by these previous remarks. As argued below, we identify the striking phenomenon as a surface-induced phase transition occurring within the nanometer-sized pores. The theoretical analysis in our earlier work[11] was made only for a very low ion concentration which was far from the threshold argued in the present work.

IV. THEORETICAL ANALYSES

A. Analysis on phase transition in bulk fluid or liquid mixture

The concepts of the phase transition of a pure fluid[12–16] or a liquid mixture[17–19] in the bulk have already been established on the basis of the integral equation theories using the hypernetted-chain (HNC) and Percus-Yevick (PY) approximations. As an example system, let us consider a pure bulk fluid, wherein the fluid particles interact through Lennard-Jones potential, at a sufficiently low temperature.[12,14] The Fourier transform of the total correlation function $h(r)$, $H(k)$, is expressed by

$$H(k) = 4\pi \int_0^\infty r^2 h(r)\{\sin(kr)/(kr)\}dr. \tag{1a}$$

$H(0)$ ($H(k)$ at zero wave vector ($k = 0$)),

$$H(0) = 4\pi \int_0^\infty r^2 h(r)dr, \tag{1b}$$

is an important parameter: When the number density ρ is gradually increased from a gas-phase value, at a threshold $\rho_G{}^*$, $H(0)$ exhibits an abrupt increase toward an extremely large value. That is, $h(r)$ becomes long ranged. When ρ is gradually decreased from a liquid-phase value, qualitatively the same behavior is observed at a threshold $\rho_L{}^*$. It is not quite definite whether at the threshold $H(0)$ truly diverges (the divergence of $H(0)$, which is equivalent to that of the isothermal compressibility or the correlation length, implies that $h(r)$ becomes infinitely long ranged) or remains finite, because the integral equation theory is solved not analytically but numerically. In either case, however, the abrupt increase can well be qualified as a signal of the spinodal instability: In the region, $\rho_G{}^* < \rho < \rho_L{}^*$, the fluid cannot exist as a single phase even in a metastable state; and the thresholds are the spinodal points for the liquid-gas phase separation beyond which the second phase unavoidably appears. In the real system, the transition occurs at a number density lower than $\rho_G{}^*$ ($\rho_G{}^+$) or higher than $\rho_L{}^*$ ($\rho_L{}^+$) ($\rho_G{}^+ < \rho < \rho_G{}^*$ and $\rho_L{}^* < \rho < \rho_L{}^+$ are the metastable regions). When the temperature is sufficiently high, there is no transition occurring.

We then consider a two-component liquid mixture[17–19] which is immiscible unless the concentration of one of the components is sufficiently low (e.g., a mixture of water and cyclohexane). When the concentration of component 1 is gradually increased from zero, at a threshold $C_1{}^*$ the Fourier transforms of the total correlation functions for the like pairs at zero wave vector ($H_{11}(0)$ and $H_{22}(0)$) simultaneously exhibit abrupt increases toward extremely large values (the Fourier transforms of the total correlation function for the unlike pair at zero wave vector, $H_{12}(0)$, displays an abrupt decrease toward an extremely large, negative value).[19] Qualitatively the same behavior is encountered at a threshold $C_2{}^*$ when the concentration of component 2 is gradually increased from zero. This *divergent* behavior, though it may not be a true divergence, gives a signal of the spinodal instability: The thresholds, $C_1{}^*$ and $C_2{}^*$, are the spinodal points for the demixing (liquid-liquid phase separation) beyond which the second phase unavoidably appears.

B. Analysis on surface-induced phase transition

The well-established concept for the phase transition of a pure fluid or a liquid mixture in the bulk has been extended by Kinoshita[20–25] to a surface-induced phase transition using some different versions of the integral equation theory (IET) combined with simple-liquid models. A very large spherical particle (this is referred to as "macroparticle") is usually employed to mimic an extended surface. In the simple-liquid model, the potential is dependent only on the distance between centers of two particles. The surface-induced phase transition is most likely to occur for water containing a low concentration of hydrophobic solute near a hydrophobic surface or for nonpolar liquid containing a low concentration of hydrophilic solute near a hydrophilic surface. The concentration of hydrophobic solute is enriched near the surface in the former while the concentration of hydrophilic solute is enriched near the surface in the latter. As the solute concentration in the bulk C increases, the enrichment becomes stronger, but the thickness of the enriched layer is microscopic in the sense that it is comparable with the solute size. However, near a threshold value of C, C^*, the Fourier transform of the surface-solute total correlation function at zero wave vector exhibits an abrupt increase toward infinity. (Since the integral equation theory is numerically solved, the abrupt increase may not be a true divergence but the behavior is highly divergent.) This can be identified as a signal of a transition phenomenon, a sudden growth of the enriched layer: The thickness of the layer grows from a microscopic scale to a submicroscopic one (much larger than the solute size but not a macroscopic scale because the bulk is thermodynamically stable as a single phase), and the solute concentration within the layer becomes much higher. This transition is referred to as the *partial-wetting transition* representing the partial wetting of the surface by the solute.[20,21,25,26] C^* is the spinodal point beyond which the liquid near the surface cannot exist as a single phase even as a metastable state. The second phase unavoidably appears at the surface. Beyond C^* the IET possesses no solutions. In the real system, the transition occurs at a concentration (C^+) that is lower than C^* ($C^+ < C < C^*$ is the metastable region). Let the thickness of the second phase be δ. The average solute concentration in the second phase and δ should be increasing functions of $C > C^*$ though they cannot be calculated by the IET.[25] The analysis on the partial-wetting transition has been extended to a molecular liquid near a surface.[26]

The physical quantity, whose gradual increase eventually gives rise to the spinodal behavior, is not necessarily the solute concentration. For example, in the case of water containing a low concentration of hydrophobic solute near a surface, it can be the degree of the surface hydrophobicity. The spinodal point is encountered when the surface hydrophobicity is gradually strengthened, if the solute concentration is sufficiently high. When the HNC closure neglecting the bridge function is employed, however, it is often that the IET looses its solutions before the Fourier transform of the surface-solute total correlation function at zero wave vector exhibits the divergent behavior: It displays a significantly large increase but no abrupt increase toward infinity; and it certainly remains finite at the threshold.[13,15,16] Thus, the HNC closure is often incapable of reproducing the spinodal behavior completely. Nevertheless, the significantly large increase accompanying the loss of the solutions can doubtlessly be regarded as a signal of the transition phenomenon (see the last paragraph in Sec. V B).

When the liquid is confined between two surfaces, if the surface separation L is sufficiently small, the confined domain is unavoidably filled with the second phase beyond a threshold value of C, C^{**}, which is referred to as the *bridging transition* (the two enriched layers bridge each other).[22–25] In the case of $L \sim 2\delta$, the spinodal point of the bridging transition C^{**} is approximately equal to C^*: $C^{**} \sim C^*$. For $L < 2\delta$, however, it is lower than C^*; it becomes lower as L decreases; and for very small L, the transition occurs at a remarkably low solute concentration in the bulk. It should be noted that the transition phenomenon is induced by the surface. As the pore diameter decreases, the liquid confined within the pore is more influenced by the surface properties. It can thus be understood and has been verified by theoretical analyses that the surface-induced transition can occur more readily for a smaller pore. We emphasize that the surface-induced phase transition occurs even when the bulk is quite stable as a single phase. As a striking example, a nanopore (a pore whose diameter is a scale of a few nanometers) can be filled with the second phase at an unexpectedly low solute concentration in the bulk.

The concept of the surface-induced phase transition proposed by Kinoshita[20–26] has been supported by a computer-simulation study. By using grand canonical Monte Carlo simulations, Greberg and Patey[27] verified the occurrence of the bridging transition for model systems mimicking water containing a low concentration of hydrophobic solute confined between hydrophobic surfaces and nonpolar liquid containing a low concentration of water confined between hydrophilic surfaces. In our view, the following experimental result is relevant to the concept. Kurihara and co-workers[28] studied cyclohexane-ethanol binary liquid near a single silica surface. Their system corresponds to nonpolar liquid (cyclohexane) containing a low concentration of hydrophilic solute (ethanol) near a hydrophilic surface (silica surface). They gradually increased the ethanol concentration from zero: They observed an abrupt formation of an ethanol layer whose thickness reached $\sim$15 nm at the ethanol concentration of $\sim$0.1 mol%. This manifests the existence of the partial-wetting transition.

C. Angle-dependent integral equation theory for molecular liquid near a surface

It is crucial to adopt a molecular model for water in the investigation of the ion-size effects. A water molecule is modeled as a hard sphere with diameter $d_S = 0.28$ nm in which a point dipole and a point quadrupole of tetrahedral symmetry are embedded.[29,30] The influence of molecular polarizability of water is included by employing the self-consistent mean field (SCMF) theory.[29,30] At the SCMF level the many-body induced interactions are reduced to pairwise additive potentials involving an effective dipole moment. Hard spherical

cations and anions with diameters d_+ and d_-, respectively, are immersed in our model water. The water-water and water-ion correlations are then dependent not only on the distance between centers of the particles but also on the orientations of water molecules. We analyze the structure of aqueous electrolyte solution at an extended, uncharged or only weakly charged (hydrophobic) surface. The water-surface correlations are also dependent on the orientations of water molecules.

We employ the angle-dependent integral equation theory (ADIET), a statistical-mechanical theory for molecular liquids.[26,29–45] A large, spherical particle with diameter $d_L = 30d_S$ mimicking an extended surface is immersed in our model aqueous electrolyte solution. The subscripts, "S," "+," "−," and "L," respectively, represent "solvent (water)," "cations," "anions," and "large particle." The large particle carries the charge Q_L placed at its center (the surface charge density is $Q_L/(\pi {d_L}^2)$). The Ornstein-Zernike (OZ) equation for the mixture comprising the large particle, water molecules, cations, and anions can be written as

$$\eta_{\alpha\beta}(12) = \{1/(8\pi^2)\}\sum_{\gamma}\rho_\gamma \int c_{\alpha\gamma}(13)\{\eta_{\gamma\beta}(32) + c_{\gamma\beta}(32)\}d(3), \tag{2a}$$

$$\eta_{\alpha\beta}(12) = h_{\alpha\beta}(12) - c_{\alpha\beta}(12);\ \alpha, \beta = \mathrm{S}, +, -, \mathrm{L}, \tag{2b}$$

where h and c are the total and direct correlation functions, respectively, (ij) represents $(\boldsymbol{r}_{ij}, \boldsymbol{\Omega}_i, \boldsymbol{\Omega}_j)$, $\boldsymbol{r}_{ij}$ is the vector connecting the centers of particles i and j, $\boldsymbol{\Omega}_i$ denotes the three Euler angles describing the orientation of particle i, $\int d(3)$ represents integration over all position and angular coordinates of particle 3, and ρ is the number density. The closure equation is expressed by

$$c_{\alpha\beta}(12) = \int_{r_{12}}^{\infty}[h_{\alpha\beta}(12)\partial\{w_{\alpha\beta}(12) - b_{\alpha\beta}(12)\}/\partial r'_{12}]dr'_{12} - u_{\alpha\beta}(12)/(k_B T) + b_{\alpha\beta}(12), \tag{3a}$$

$$w_{\alpha\beta}(12) = -\eta_{\alpha\beta}(12) + u_{\alpha\beta}(12)/(k_B T), \tag{3b}$$

where u is the pair potential, b is the bridge function, and $r_{12} = |\boldsymbol{r}_{12}|$. In the present analysis, the HNC approximation is employed ($b = 0$). We assume that the macroparticle is present at infinite dilution ($\rho_L \to 0$). The calculation process can then be split into two steps:

Step (i). Solve Eqs. (2a)–(3b) for bulk aqueous electrolyte solution. Calculate the correlation functions X_{SS}, X_{S+}, X_{S-}, X_{++}, X_{+-}, and X_{--} ($X = h, c$).

Step (ii). Solve Eqs. (2a)–(3b) for the macroparticle-aqueous electrolyte solution system using the correlation functions obtained in step (i) as input data. Calculate the correlation functions X_{LS}, X_{L+}, and X_{L-} ($X = h, c$).

For the numerical solution of Eqs. (2a)–(3b), the pair potentials and correlation functions are expanded in a basis set of rotational invariants (i.e., Wigner's generalized spherical harmonics), and the basic equations are reformulated in terms of the projections $X^{mnl}_{\mu\nu}(r)$ (r is the distance between centers of two particles) occurring in the rotational-invariant expansion of X. The expansion considered for $m, n \le n_{max} = 4$ gives sufficiently accurate results. The basic equations are then numerically solved using the robust, highly efficient algorithm developed by Kinoshita and co-workers.[35,37] In the numerical treatment, a sufficiently long range r_L is divided into N grid points ($r_i = i\delta r$, $i = 0, 1, \ldots, N-1$; $\delta r = r_L/N$) and all of the projections are represented by their values on these points. The grid width and the number of grid points are set at $\delta r = 0.01 d_S$ and $N = 4096$, respectively.

In the real system treated in the present study, the solution is confined within pores having various sizes whose surfaces are concave. However, the analyses on the solution confined by an extended surface provide fundamental information which can readily be applied to the solution confined between two extended surfaces, between two concave surfaces, or within a nanopore in a semi-quantitative sense. The microstructure (heterogeneity) of the surface is not taken into account in the theoretical calculation. However, it has been shown that it has no essential effects on the conclusion as long as the *averaged* properties of the surface-induced structure are discussed.[46]

The aqueous electrolyte solution in the present system is modeled as follows. It is treated as water containing K_2PtCl_4 or K_2PtBr_4 at C M. The anion (i.e., the platinum complex ion), $[PtCl_4]^{2-}$ or $[PtBr_4]^{2-}$, is modeled as a spherical ion within which the point charge of $-2e$ (e is the elementary electric charge) is placed at the center. The point charge of K^+ placed at its center is e. The cation size d_+ is set at 0.3 nm. As the anion size d_-, 0.60 nm is adopted for $[PtCl_4]^{2-}$. The size of $[PtCl_4]^{2-}$ was approximately calculated from the molecular weight and density of K_2PtCl_4 in solid state with the tetragonal crystal structure. The size difference between $[PtBr_4]^{2-}$ and $[PtCl_4]^{2-}$ can be set at the double of the size difference between Br^- and Cl^-, with the result that $d_- = 0.70$ nm is adopted for $[PtBr_4]^{2-}$.[47] A cation and an anion carry the charges e and $-2e$, respectively, and $\rho_+ = 2\rho_-$.

The versatility and reliability of the ADIET was demonstrated in our earlier works. For example, the hydration free energies of nonpolar solutes calculated by the ADIET with the multipolar model are in quantitatively excellent agreement with those from Monte Carlo computer simulations.[43] The dielectric constant of bulk water calculated, which is a good measure of the validity of a molecular theory, is ∼83 that is in good accord with the experimental value ∼78. The ADIET has successfully been applied to detailed analyses on bulk water and aqueous electrolyte solution,[29,30] electrical double-layer,[31–34] water or aqueous electrolyte solution near a hydrophobic surface,[35,38,40–42] interaction between colloidal particles in aqueous electrolyte solution,[36] metal-aqueous electrolyte solution interface,[39] negative heat capacity of hydrophilic hydration,[45] weakening of the hydrophobicity at low temperatures,[48] and rotational component of (i.e., contribution from the restriction of rotational freedom of water molecules near the solute to) the hydration entropy.[44]

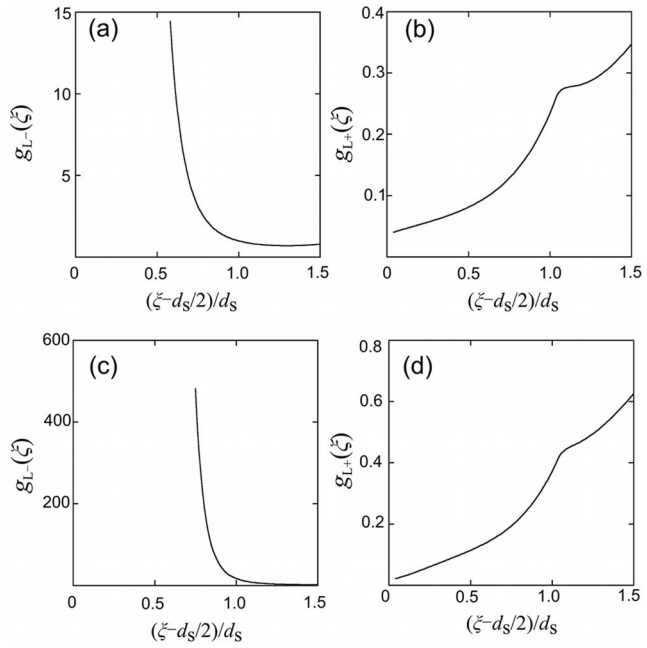

FIG. 4. Normalized number-density profiles of anions $g_{L-}(\xi)$ (a) and (c) and cations $g_{L+}(\xi)$ (b) and (d) near an extended hydrophobic surface for $d_- = 0.60$ nm (a) and (b) and $d_- = 0.70$ nm (c) and (d). The anions are platinum complex ions, $[PtCl_4]^{2-}$ or $[PtBr_4]^{2-}$, and the cations are potassium ions, K^+. $d_- = 0.60$ nm and $d_- = 0.70$ nm correspond to $[PtCl_4]^{2-}$ and $[PtBr_4]^{2-}$, respectively. It is indicated that the anion concentration is enriched near the surface whereas the cations are depleted.

D. Application to the present system, aqueous electrolyte solution near a hydrophobic surface: A surface-induced layer whose thickness is comparable with anion size

First, we show $g_{L+}(\xi)$ (ξ is the distance from the surface) as well as $g_{L-}(\xi)$ near a hydrophobic surface ($Q_L = 0$) in Figure 4. C is set at 0.005 M that is much lower than the spinodal concentration. The two values, 0.60 nm and 0.70 nm, are tested for d_-. The concentration of anions (i.e., platinum complex ions) is enriched in the immediate vicinity of the surface. As discussed in our recent publication,[11] the anions are not strongly hydrated due to the large anion size despite that the charge carried by them is as large as $-2e$. As a consequence, the anions are excluded from the bulk to the surface. This effect is stronger for $[PtBr_4]^{2-}$ than for $[PtCl_4]^{2-}$: The degree of the enrichment is remarkably sensitive to the anion size. By contrast, the cations are highly hydrophilic due to their small size and they are preferentially and strongly hydrated in the bulk, with the result that they are depleted near the surface. Of course, the local charge neutrality does not hold near the surface.

The strong enrichment of the anion concentration occurs only within the first layer, $0 \le (\xi - d_-/2)/d_S < 1$. $g_{L-}(\xi)$ reduces quite rapidly as ξ increases. In this sense, the layer within which the anion concentration is enriched is microscopic. Our experience in analyses on confined aqueous electrolyte solutions has shown the following. Let us consider the solution confined between two extended surfaces. When the surface separation L is not small, the solution around the center is very much like that in the bulk and the normalized number-density profile of anions near each of the surfaces is close to that near a single surface. As L becomes smaller, the solution for all ξ is more influenced not only by the nearest surface but also by the other surface. When L becomes smaller than a few times of the diameter of a water molecule, the normalized number-density profile for all ξ exhibits an upward shift and the anion-size effect becomes larger. As discussed in our recent publication, the upward shift and the enhancement of anion-size effect are more appreciable when L is smaller or the surface is concave and its curvature is larger. By the interplay of these physical factors, the enrichment of anion concentration and the anion-size effect become larger when the solution is confined within a pore having the size of a nanometer.

E. Partial-wetting transition in the present system

In order to investigate the partial-wetting transition in the present system, we monitor the two quantities, $g_{L-}(d_-/2)$ and $H_{L-}(0)$. Here, $g_{L-}(\xi) = \rho_{L-}(\xi)/\rho_-$ where ξ is the distance from the surface, $\rho_{L-}(\xi)$ is the number-density profile of anions, and ρ_- is the number density of anions in the bulk. $g_{L-}(\xi)$ represents the surface-induced hydration structure of anions and $g_{L-}(\xi) \to 1$ as $\xi \to \infty$. $H_{L-}(k)$ is the Fourier transform of $h_{L-}(r)$ ($g_{L-}(r) = h_{L-}(r)+1$)

$$H_{L-}(\mathrm{k}) = 4\pi \int_0^\infty r^2 h_{L-}(r)\{\sin(kr)/(kr)\}dr. \tag{4a}$$

$H_{L-}(0)$ expressed by

$$H_{L-}(0) = 4\pi \int_0^\infty r^2 h_{L-}(r)dr \tag{4b}$$

gives a signal of the transition phenomenon as described above, but $g_{L-}(d_-/2)$ also gives an equivalent signal.

The theoretical analysis is made for the partial-wetting transition near a single, extended hydrophobic surface. Figure 5 shows the plot of $g_{L-}(d_-/2)$ or $H_{L-}(0)$ against the anion concentration in the bulk denoted by C. The two values, 0.60 nm ($[PtCl_4]^{2-}$) and 0.70 nm ($[PtBr_4]^{2-}$), are tested for d_-. As observed in the figure, both $g_{L-}(d_-/2)$ and $H_{L-}(0)$ tend to diverge at $C^* \sim 0.0255$ M for $d_- = 0.60$ nm and at $C^* \sim 0.0095$ M for $d_- = 0.70$ nm. This divergent behavior is a signal of the partial-wetting transition, a sudden growth of the enriched layer from a microscopic scale to a submicroscopic one. C^* is the spinodal point (the spinodal concentration) explained above.

V. COMPARISON BETWEEN EXPERIMENTAL AND THEORETICAL RESULTS

When the ADIET combined with the molecular model for water is employed, it is difficult to directly analyze the bridging transition. However, the analysis of the partial-wetting transition provides useful information on the bridging transition as well. As argued in Sec. IV B, both the two types of transitions have been investigated (not only theoretically[20–26] but also experimentally[27,28]) in detail for the same system consisting of simple-liquid models, and the connection between them is rather straightforward.

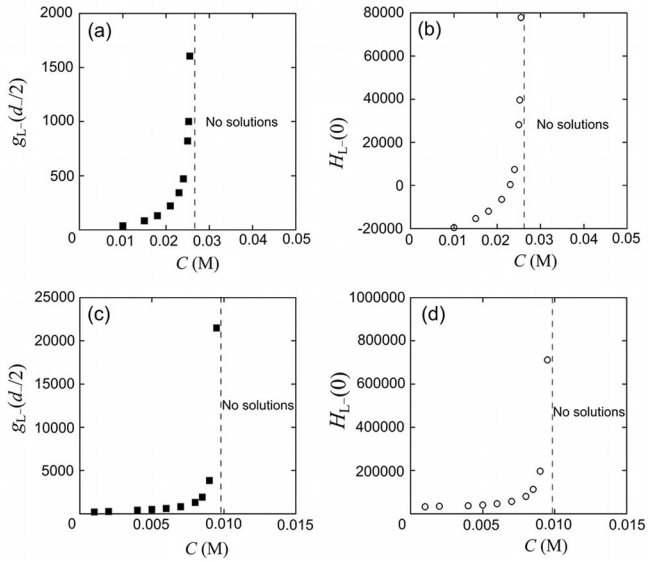

FIG. 5. Relation between $g_{L-}(d_-/2)$ (a) and (c) or $H_{L-}(0)$ (b) and (d) and C (the concentration of anions, platinum complex ions) near an extended hydrophobic surface for $d_- = 0.60$ nm (a) and (b) and $d_- = 0.70$ nm (c) and (d). $d_- = 0.60$ nm and $d_- = 0.70$ nm correspond to $[PtCl_4]^{2-}$ and $[PtBr_4]^{2-}$, respectively. Both $g_{L-}(d_-/2)$ and $H_{L-}(0)$ diverge at $C^*\sim 0.0255$ M for $d_- = 0.60$ nm and at $C^*\sim 0.0095$ M for $d_- = 0.70$ nm. Beyond C^* (in the region indicated by "no solutions"), the theory possesses no solutions.

A. Threshold for concentration of platinum complex ions (anion concentration) in bridging transition

The spinodal concentration for the partial-wetting transition is $C^*\sim 0.0255$ M for $[PtCl_4]^{2-}$ and at $C^*\sim 0.0095$ M for $[PtBr_4]^{2-}$. The pore diameter of our porous silicon is ~3 nm on the average. The spinodal concentration for the bridging transition within such a narrow pore, C^{**}, should be considerably lower than C^*. The anion concentration at which the bridging transition occurs, C°, is even lower than C^{**}. The threshold values observed in our experiments, ~0.0095 M for $[PtCl_4]^{2-}$ and ~0.0045 M for $[PtBr_4]^{2-}$, correspond to C°. Thus, the theoretical results are in agreement with the experimental observations in a semi-quantitative sense.

B. Threshold for affinity of pore-wall surface with water (strength of surface hydrophobicity) in bridging transition

By fixing C at 0.0260 M for $d_- = 0.60$ nm ($[PtCl_4]^{2-}$; $C > C^*$), we analyze the effect of Q_L (this is a negative quantity) on $g_{L-}(d_-/2)$ or $H_{L-}(0)$. The essential matter is to set C at a value higher than C^*. Q_L is a measure of the hydrophobicity of the surface. As Q_L becomes closer to zero, the surface hydrophobicity becomes stronger. We gradually increase Q_L from the initial value, $-100e$. Figure 6 shows the plot of $g_{L-}(d_-/2)$ or $H_{L-}(0)$ against Q_L. Both $g_{L-}(d_-/2)$ and $H_{L-}(0)$ continue to increase until $Q_L\sim -50e$ though the increases are not divergent. For $Q_L > -50e$, the ADIET possesses no solutions. This result is indicative that the partial-wetting transition occurs beyond threshold strength of the surface hydrophobicity, which is qualitatively consistent with the experimental result.

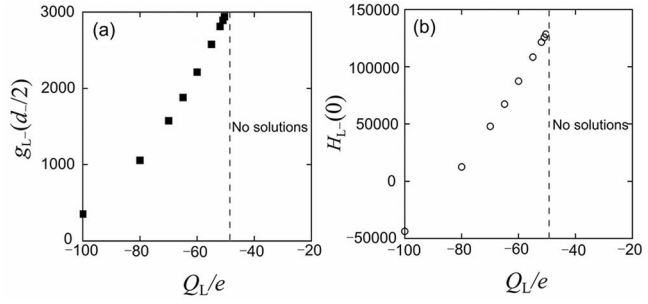

FIG. 6. Relation between $g_{L-}(d_-/2)$ (a) or $H_{L-}(0)$ (b) and Q_L/e (e is the elementary electric charge) near an extended surface for $d_- = 0.60$ nm corresponding to $[PtCl_4]^{2-}$. $|Q_L/e|$ is a measure of strength of hydrophobicity of the surface: Smaller $|Q_L/e|$ implies weaker hydrophobicity. Both $g_{L-}(d_-/2)$ and $H_{L-}(0)$ continue to increase, but beyond $Q_L/e \sim -50$ (in the region indicated by "no solutions"), the theory possesses no solutions.

C. Properties of the second phase

The second phase appearing in the present system comprises the anions, water molecules, and cations. The anion concentration in the second phase should be orders of magnitude higher than C. Water molecules and cations are required for screening the electrostatic repulsive interactions among the anions. In fact, near the spinodal concentration C^*, $g_{LS}(d_S/2)$ and $g_{L+}(\xi)$ ($\xi\sim d_- + d_+/2$) also exhibit rather abrupt increases. The peaks of $g_{L-}(d_-/2)$ and $g_{L+}(d_- + d_+/2)$ are indicative that the cations preferentially come into contact with the anions. The abrupt increase in $g_{L-}(d_-/2)$ is more striking for $[PtBr_4]^{2-}$ than for $[PtCl_4]^{2-}$, implying that the anion concentration in the second phase is substantially higher for $[PtBr_4]^{2-}$. This result is in marked contrast with the case of water containing a nonpolar solute near a hydrophobic surface: In this case, the partial wetting of the surface by the solute accompanies the partial drying of the surface by water; and the second phase is formed by the solute molecules almost exclusively.[23,25,26]

The ion concentration in the second phase filling a narrow pore should be much higher than that formed at a single surface. Only if the pores are filled with the second phase, the electrodeposition is drastically accelerated because it is completely free from the diffusion-limited condition. Filling a pore with the second phase takes place as long as its diameter is sufficiently small regardless of its depth, which was proved by our experimental result illustrated in Figure 3.

D. Irrelevance to mass-transfer effect

The mass-transfer efficiency is not necessarily proportional to the anion concentration especially in nanospace. However, even such nonlinear behavior is not relevant to the transition phenomena by which the second phase abruptly appears and completely fills the whole space within nanopores. The phenomena arise from the long-range nature of the surface-anion correlation length. The mass transfer, whose driving force is the concentration gradient of the anions, is incapable of reproducing such transition phenomena. It is shown in our experiments that the whole space within nanopores is abruptly filled with the second phase even when

the affinity of the surface with water is continuously reduced with fixing the ion concentration. This gives another evidence of the irrelevance to the mass-transfer effect.

E. Effect of electrochemical factors

Electrochemical factors are not taken into account in our theoretical analyses. What we have shown in the present study is as follows: Before the electrodeposition is started, the nanopores are filled with the second phase within which the anion concentration is orders of magnitude higher than in the bulk solution; and the anions are continuously supplied to the nanopores as they are consumed by the electrodeposition. The filling occurs quite rapidly just as the phase separation of a bulk liquid into two immiscible phases. The supply of the anions also occurs quite rapidly as long as the transition concentration of the anions is maintained in the bulk, which is consistent with the experimental observation that the porous layers is uniformly filled with the deposited platinum. We remark that the impact of the surface-induced phase transition is remarkable. Presumably, the surface is positively charged at the potential of platinum electrodeposition, and a positive electric field is emanated from the surface. Due to the field, the anions are attracted to the surface, acting in the direction where the transition phenomena are even enhanced. The neglect of the field is another factor leading to overestimation of C^* (see Sec. V A), but it does not vitiate the agreement between the experimental and theoretical results. Even if the surface is negatively charged, unless the surface-charge density is high, the surface-induced phase transition persists as shown in a theoretical study:[26] It persists even at weakly charged (hydrophilic) surfaces immersed in water containing a low concentration of hydrophobic solute. A statistical-mechanical theory incorporating the electric field[39] has been developed, and the application of such a theory to the present case is a task for the future.

VI. CONCLUDING REMARKS

We have found the existence of thresholds for the concentration of platinum complex ions and the affinity of the pore wall surface with water in the electrochemical deposition of platinum within silicon electrode nanopores. The drastic change in the deposition behavior, which is exhibited beyond the threshold, cannot be explained by the consideration of the electrochemical reaction coupled with mass transfer. Also, the enrichment of the ion concentration within a thin layer at the surface is not capable of elucidating the drastic change, either. With the aid of statistical-mechanical theory for confined molecular liquids, we have revealed that the drastic change originates from a surface-induced phase transition. In our case, it occurs when the pore wall surface is sufficiently hydrophobic and the ion size is large enough for the ions to exhibit rather hydrophobic properties. As the ion size increases, for a fixed ion concentration the transition occurs even within larger pores, and for a fixed pore size it occurs at lower ion concentration in the bulk. Upon the transition, the nanopores are filled with the second phase within which the ion concentration is orders of magnitude higher than in the bulk. The problem of the diffusion-limited condition, under which supply of the ions from the bulk becomes difficult, is completely overcome by the transition phenomenon. Once sufficiently large nuclei of platinum are formed on the electrode surface, the electrodeposition proceeds quite easily.

A surface-induced phase transition in nanospace was predicted by previous theoretical studies.[20–27,49,50] Also, an experimental result[28] which should be relevant to the transition phenomenon is found in the literature. However, it has been investigated, for the first time, for the same system from both experimental and theoretical viewpoints in the present study. Moreover, its occurrence has never been reported for an aqueous electrolyte solution near a hydrophobic surface, which contains only weakly hydrated ions. It is interesting to look at some more different aqueous electrolyte solutions in future studies. Although the nanoporous materials have become important platforms for electrochemical reactions, the mass transfer of chemicals to and within nanopores has not yet been understood as emphasized in a recent review.[51] A surface-induced phase transition can take place even when the bulk liquid mixture is thermodynamically stable as a single phase, and it should be one of the crucial factors for controlling the electrochemical reactions that is substantially different from the mass transfer. It can be applied to other chemical reactions within nanometer-sized porous media: The transition filling nanospace with a solution containing reactants at orders of magnitude higher concentration will enable us to design and control novel materials possessing nanoporous structure. At the same time, the present results will stimulate the pioneering work in an interesting field for a liquid or liquid mixture confined in nanospace.

ACKNOWLEDGMENTS

R.K. is grateful to the Global COE program, "Energy Science in the Age of Global Warming." This work was supported by Grant-in-Aid for Young Scientists (B) (No. 23750239) and that for Scientific Research on Innovative Areas (No. 20118004) from the Ministry of Education, Culture, Sports, Science and Technology of Japan.

[1] M. P. Schwartz, S. D. Alvarez, and M. J. Sailor, Anal. Chem. **79**, 327 (2007).
[2] M. M. Orosco, C. Pacholski, and M. J. Sailor, Nat. Nanotechnol. **4**, 255 (2009).
[3] Y. Yamauchi, A. Sugiyama, R. Morimoto, A. Takai, and K. Kuroda, Angew. Chem., Int. Ed. **47**, 5371 (2008).
[4] R. Nakamura and H. Frei, J. Am. Chem. Soc. **128**, 10668 (2006).
[5] H. Föll, J. Carstensen, E. Ossei-Wusu, A. Cojocaru, E. Quiroga-Gonzalez, and G. Neumann, J. Electrochem. Soc. **158**, A580 (2011).
[6] M. Leisner, A. Cojocaru, E. Ossei-Wusu, J. Carstensen, and H. Föll, Nanoscale Res. Lett. **5**, 1502 (2010).
[7] K. Fukami, Y. Tanaka, M. L. Chourou, T. Sakka, and Y. H. Ogata, Electrochim. Acta **54**, 2197 (2009).
[8] R. M. Lynden-Bell, A. I. Frolov, and M. V. Fedorov, Phys. Chem. Chem. Phys. **14**, 2693 (2012).
[9] A. I. Frolov, K. Kirchner, T. Kirchner, and M. V. Fedorov, Faraday Discuss. **154**, 235 (2012).
[10] A. I. Frolov, R. N. Arif, M. Kolar, A. O. Romanova, M. V. Fedorov, and A. G. Rozhin, Chem. Sci. **3**, 541 (2012).
[11] K. Fukami, R. Koda, T. Sakka, T. Urata, K. Amano, H. Takaya, M. Nakamura, Y. Ogata, and M. Kinoshita, Chem. Phys. Lett. **542**, 99 (2012).

[12]J. J. Brey and A. Santos, J. Chem. Phys. **82**, 4312 (1985).
[13]M. Kinoshita and M. Harada, Mol. Phys. **65**, 599 (1988).
[14]E. Lomba, Mol. Phys. **68**, 87 (1989).
[15]L. Belloni, J. Chem. Phys. **98**, 8080 (1993).
[16]G. Sarkisov and E. Lomba, J. Chem. Phys. **122**, 214504 (2005).
[17]G. Malescio, J. Chem. Phys. **95**, 1198 (1991).
[18]X. S. Chen, M. Kasch, and F. Forstmann, Phys. Rev. Lett. **67**, 2674 (1991).
[19]C. P. Ursenbach and G. N. Patey, J. Chem. Phys. **100**, 3827 (1994).
[20]M. Kinoshita, Mol. Phys. **94**, 485 (1998).
[21]M. Kinoshita, Mol. Phys. **96**, 71 (1999).
[22]M. Kinoshita, Chem. Phys. Lett. **325**, 281 (2000).
[23]M. Kinoshita, Chem. Phys. Lett. **326**, 551 (2000).
[24]M. Kinoshita, Chem. Phys. Lett. **333**, 217 (2001).
[25]M. Kinoshita, "Surface-induced phase transition and long-range surface force: Roles in colloidal and biological systems," *Recent Research Developments in Molecular Physics* (Transworld Research Network, India, 2003), Vol. 1, pp. 21–41.
[26]M. Kinoshita, J. Solution Chem. **33**, 661 (2004).
[27]H. Greberg and G. N. Patey,J. Chem. Phys. **114**, 7182 (2001).
[28]M. Mizukami, M. Moteki, and K. Kurihara, J. Am. Chem. Soc. **124**, 12889 (2002).
[29]P. G. Kusalik and G. N. Patey, J. Chem. Phys. **88**, 7715 (1988).
[30]P. G. Kusalik and G. N. Patey, Mol. Phys. **65**, 1105 (1988).
[31]G. M. Torrie, P. G. Kusalik, and G. N. Patey, J. Chem. Phys. **89**, 3285 (1988).
[32]G. M. Torrie, P. G. Kusalik, and G. N. Patey, J. Chem. Phys. **90**, 4513 (1989).
[33]G. M. Torrie, P. G. Kusalik, and G. N. Patey, J. Chem. Phys. **91**, 6367 (1989).
[34]G. M. Torrie and G. N. Patey, J. Phys. Chem. **97**, 12909 (1993).
[35]M. Kinoshita and M. Harada, Mol. Phys. **81**, 1473 (1994).
[36]M. Kinoshita, S. Iba, and M. Harada, J. Chem. Phys. **105**, 2487 (1996).
[37]M. Kinoshita and D. R. Bérard, J. Comput. Phys. **124**, 230 (1996).
[38]N. M. Cann and G. N. Patey, J. Chem. Phys. **106**, 8165 (1997).
[39]D. R. Bérard, M. Kinoshita, N. M. Cann, and G. N. Patey, J. Chem. Phys. **107**, 4719 (1997).
[40]M. Kinoshita, J. Mol. Liq. **119**, 47 (2005).
[41]M. Kinoshita, N. Matubayasi, Y. Harano, and M. Nakahara, J. Chem. Phys. **124**, 024512 (2006).
[42]M. Kinoshita, Condens. Matter Phys. **10**, 387 (2007).
[43]M. Kinoshita, J. Chem. Phys. **128**, 024507 (2008).
[44]M. Kinoshita and M. Suzuki, J. Chem. Phys. **130**, 014707 (2009).
[45]M. Kinoshita and T. Yoshidome, J. Chem. Phys. **130**, 144705 (2009).
[46]J. C. Shelley, G. N. Patey, D. R. Bérard, and G. M. Torrie, J. Chem. Phys. **107**, 2122 (1997).
[47]M. Kinoshita and F. Hirata, J. Chem. Phys. **106**, 5202 (1997).
[48]T. Yoshidome and M. Kinoshita, Phys. Chem. Chem. Phys. **14**, 14554 (2012).
[49]K. Kiyohara, T. Sugino, and K. Asaka, J. Chem. Phys. **134**, 154710 (2011).
[50]K. Kiyohara, H. Shinoyama, T. Sugino, and K. Asaka, J. Chem. Phys. **136**, 094701 (2012).
[51]J. H. Bae, J. H. Han, and T. D. Chung, Phys. Chem. Chem. Phys. **14**, 448 (2012).